EASR

Engineering and Applied Science Research

https://www.tci-thaijo.org/index.php/easr/index

Published by the Faculty of Engineering, Khon Kaen University, Thailand

Correlation between erosion and energy consumption of sandstones

Sarusa Patanapongsonti, Laksikar Sitthimongkol*, Thanittha Thongprapha and Kittitep Fuenkajorn

Geomechanics Research Unit, Institute of Engineering, Suranaree University of Technology, Nakhon Ratchasima 30000, Thailand

Received 1 April 2024
Revised 11 September 2024
Accepted 7 October 2024

Abstract

This study aims at simulating rock erosion by slake durability testing under wet and dry conditions. Phra Wihan sandstone and conglomeratic and bedded sandstones from Phu Phan formation are used as rock specimens. The test parameters are modified from the standard to accelerate the erosion process, where 2,000 drum revolutions are used instead of 200 revolutions for up to 80 test cycles (80 days). Results indicate that fragment roundness and sphericity increase with test cycles. Bedding planes reduce the roundness of bedded sandstone as the fragments become smaller. Phra Wihan sandstone is physically insensitive to water. The water-sensitive and soft Phu Phan sandstone, however, shows notable increases of porosity and reduction of density under both wet and dry conditions. Scrubbing and colliding processes mainly reduce the fragment sizes, under dry condition. Under submerging condition, even though fragment weight is decreased by its buoyancy force, intergranular bonding of the two Phu Phan sandstones is weakened by water penetration, leading to higher percentage of passing materials and lower energy required to disintegrate the rocks than under dry condition. Water insensitive Phra Wihan sandstone erodes more quickly under dry condition than under wet condition. Even though it requires longer period to erode under water submersion, due to buoyancy force, it consumes less energy than those under dry condition to reach the same fragment sizes. Larger sandstone fragments use energy more efficiently to reduce their size than the smaller ones.

Keywords: Slake durability, Roundness, Sphericity, Water penetration, Intergranular bonding

1. Introduction

Rock degradation or erosion is a process affecting mechanical stability of slope embankments and underground excavations. It also involves long-term evolution of earth topography. Prediction of the erosion rate is, therefore, important for determining the stability of the above geological structures. Several erosional factors for rock have been studied during the past decades, where they are generally classified as external and internal factors. Sibille et al. [1] and Flore et al. [2] define that external factors involve dynamics energy induced by water flow, wind blow, rainfall, evaporation, and climatic erosivity. The internal factors involve rock texture, surface roughness, mineral alteration, density, porosity, and mineral durability [3-7]. As a results different rock types show different degradation rates controlling by their physical, chemical, and mechanical properties [8].

Some investigators define that erosion is one of the processes that governing the degradation behavior of rock. This process occurs through various mechanisms. It requires dynamic force within rock itself to cause the detachment (weathering) and the external forces to transport in an environment systems [9, 10]. Foye [11] delineates two different mechanisms in the process: (1) mechanical erosion (corrasion) and (2) chemical erosion (corrosion). These mechanisms work in a similar way in the weathering process. The mechanical erosion requires motion of atmospheric action, and chemical erosion occurs to alter the internal components within rocks though action of chemical agents that present in the transporting environments.

The slake durability index test is one of the techniques for rock durability assessment and indicate the capacity of rock degradation in laboratory conditions. Nichols [12] reports that the resistance to erosion can be described in terms of durability parameters. One of the most prevalent method is slake durability index (SDI) testing, as specified by the American Society for Testing and Materials [13]. The determination and classification of SDI have widely been developed to correlate the degrees of deterioration among different rock types [5, 14-16]. To predict long-term behavior, number of cycles of heating-drying is increased from the standard specifications, which allows correlating rock properties with long-term durability [6, 17, 18]. The correlation coefficient for their relationships increases with increasing number of test cycles. Torsangtham et al. [19] find that for sedimentary rocks in Khorat group, the greater number of test cycles causes the intergranular bonding to become weakening and developing microcracks. Fereidooni and Khajevand [20] and Walsri et al. [21] conclude from their test results that the reduction of SDI under wet testing is greater than under dry testing. The durability index varies among different rock types, which is influenced by their physical, chemical, and mechanical properties. Sedimentary rocks that contain smectite or montmorillonite show the reduction in durability under wet testing, as a result of expansive forces [22-24]. Experimental results obtained by Sousa et al. [25] indicate that texture is one of the main factors controlling the physical and chemical alterations within the rock. The results agree with those of Corominas et al. [26] and Heidari et al. [27] who conclude that rock textures (e.g. fine-grained matrix, clastic framework, and cementing agent), affect degradation process more than do mineral

*Corresponding author.
Email address: laksikar.lak2014@gmail.com
doi: 10.14456/easr.2024.65

compositions. Hawkins and McConnell [28] find that ferruginous cementing in British Isles sandstones is mostly susceptible to water, and that chlorite also shows more critical role in strength loss than expansive clays. The energy required for rock disintegration has rarely been investigated.

While recent studies have been concentrated on the observations of in-situ degradation or weathering and rock durability simulation in laboratory, mathematical representation correlating between their physical degradation and the required energy has never been developed.

The objective of this study is to simulate the effect of erosion process under physical degradation on three Thai sandstones. The main task involves performing slake durability index test under dry and wet conditions. The test parameters are modified beyond the ASTM standard specifications to obtain results that can represent long-term durability of rock specimens. Mineralogical and physical characteristics of the specimens are considered in the analysis. The specimens durability is correlated with the energy required to induce different degrees of degradation, and hence allows predicting long-term erosion of the rocks.

2. Sample preparation

Three sandstone types have been used in this study, including Phra Wihan sandstone (PWSS), Phu Phan conglomeratic sandstone (PPCS) and bedded sandstone (PPSS). They are widely exposed in the northeast of Thailand. Murray et al. [29] give description and origin of the two formations. These rock formations host a variety of infrastructures, e.g. slope embankments, foundations of railways and roadways, and abutments of dams. The main objective is to test sandstones with a variety of textures and mineral compositions. The conglomeratic (PPCS) and bedded sandstones (PPSS) are from the lower part of Phu Phan formation. PWSS sandstone specimens are from the upper part of Phra Wihan formation. They show different petrographic characteristics. Figure 1 (upper row) gives closed-up images of rock specimens. Their petrographic images are given in Figure 1 (lower row), where PWSS shows no bedding planes, and has grain sizes ranging from 0.2 to 0.7 mm. PPCS shows an alignment of grain elongation parallel to bedding planes with grain sizes ranging from 0.1 mm to 2 cm, and the PPSS has grain sizes ranging from 0.1 to 0.5 mm. The rock density is determined in accordance with ASTM D7263-21 standard [30]. The densities are 2.35 g/cc for PWSS, 2.67 g/cc for PPCS, and 2.53 g/cc for PPSS. Twenty cubical specimens with nominal dimensions of 28×28×28 mm^3 have been prepared for each rock type. Ten specimens are used for dry slake durability index test, and the rest for wet testing (with water in trough). The combined dry weight of the ten specimens is about 500 g, following ASTM D4644-16 standard [13]. Phu Phan sandstones are prepared such that their bedding planes are parallel to one of the specimen sides. This is primarily to simulate the actual discontinuity systems found under in-situ condition where two joint sets are nearly perpendicular and normal to the bedding planes.

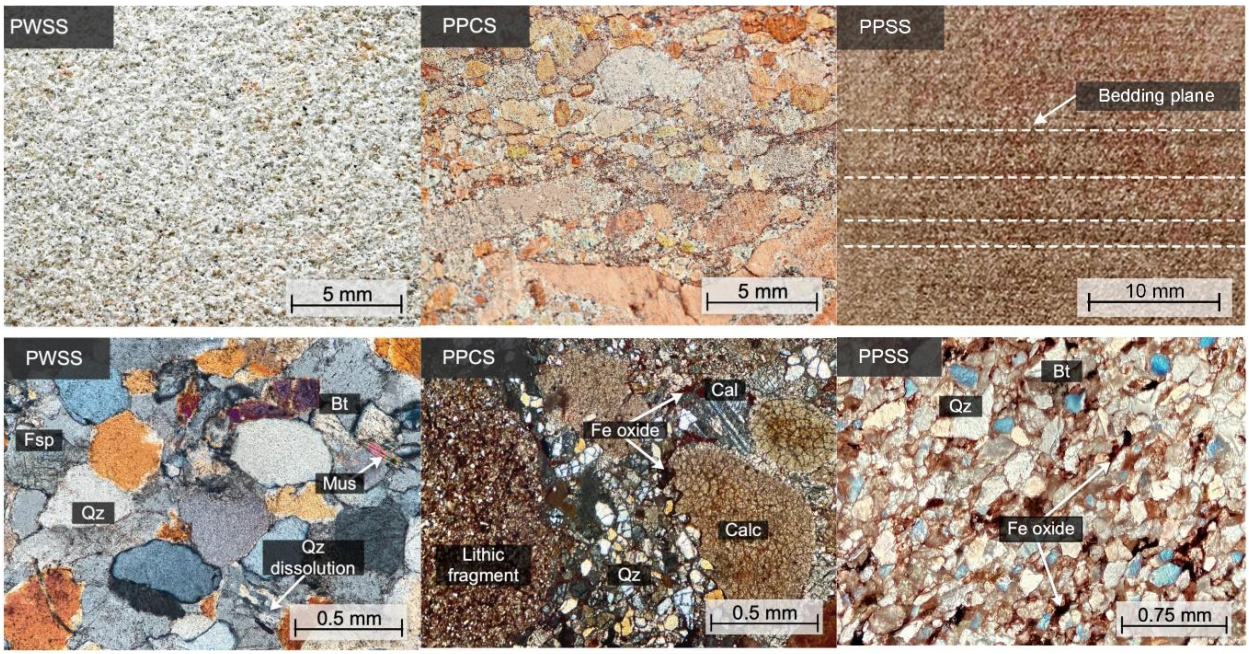

Figure 1 Closed-up images of specimens in upper row and petrographic images under cross polarized light in the row of PWSS, PPCS and PPSS. Quartz (Qz), Calcite (Cal), Calcrete (Calc), Muscovite (Ms) and Biotite (Bt)

3. Test methods

The slake durability index test procedure and calculation follow ASTM D4644-16 standard [13], except that 2,000 revolutions of drum are used for each test cycle up to 80 cycles (80 days), instead of 200 revolutions for 2 days, as specified by the standard. This is primarily to enhance the erosion process under high input energy that would occur in the field for long-period. The number of revolutions represents the maximum numbers that the test can be completed in one day. The rotational speed of each revolution is 20 rpm. Two sets of specimens for all rock types are tested: one under dry condition, the other under wet condition (with water in trough). The rock fragments remaining in the drum are oven-dried and weighted daily. Photographs of the remain fragments are taken. Particles passing the drum (with sizes of 2 mm or less) are also oven-dried and weighted. The diagram shown in Figure 2 represents one test cycle. X-ray diffraction (XRD) analysis is performed on the initial condition of rock specimens and at the end of 80 test cycles. It is performed based on the Rietveld refinement method as specified by ASTM E3294-22 standard [31]. After 80 test cycles density of the fragments remaining in the drum is determined in accordance with ASTM D7263-21 standard method [30].

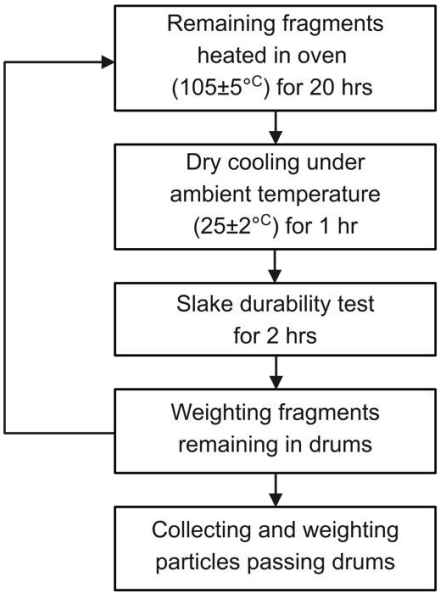

Figure 2 Diagram representing one test cycle (one day)

4. Test results

4.1 Specimen shape

Figure 3a shows representative images of the specimens prepared before testing and those remaining in the drum after subjecting to the slake durability tests under dry and wet conditions for 20, 40, 60 and 80 cycles (Figures 3b and 3c). They become rounder and smaller as the test cycles progress, where the PPSS specimens tend to be less durable than the PPCS and PWSS specimens. The roundness and sphericity of each rock fragment remaining in the drum are determined and classified based on Hryciw et al. [32]. The results are given in Figure 4, where the roundness (R) is calculated by:

$$R = (\sum_{i=1}^{n} r_i/n)/r_{ins} \quad (1)$$

where r_i is radius of circles filled to the corners of each fragment, n is number of fragment corners used in the calculation, and r_{ins} is the largest radius of circle fitted to the entire fragment. Mean and standard deviations of the roundness values after subjecting to 20, 40, 60 and 80 test cycles are shown in Figure 4a. For all rock types and test conditions, the increase of fragment roundness from very angular (R<0.17) to different roundness values is obtained. After 80 test cycles, PPSS fragments under wet condition can be classified as well rounded (R>0.7), while PPCS fragments under dry and wet conditions show only subrounded characteristics (0.35<R<0.49). The diagram suggests also that the roundness of all rock types would likely increase if the test is continued beyond 80 cycles.

Figure 3 Initial cubical specimens (a) prepared for slake durability index testing and representative images of specimens after subjected to 20, 40, 60 and 80 test cycles under dry (b) and wet (c) conditions

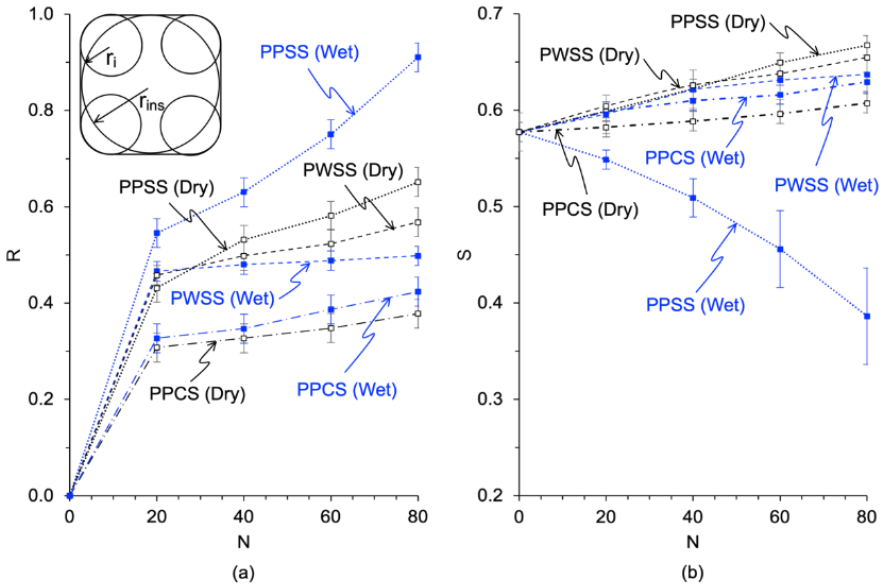

Figure 4 Fragment roundness (a) and sphericity (b) as a function of test cycle measured every 20 days, classified in accordance with Hryciw et al. [32]. Open points represent dry testing and solid points represent wet testing

The sphericity (S) of all fragments are calculated from the initial condition though 80 test cycles with 20 cycle interval, as shown in Figure 4b:

$$S = d_2/d_1 \tag{2}$$

where d_1 and d_2 represent the widest and the narrowest diameters of the fragments.

Figure 4b plots the mean and standard deviation of the sphericity values. Except for PPSS fragments under wet testing, all rock fragments show linear increases of sphericity values from the initial condition with S=0.58 to the test cycle 80 with S=0.60-0.65. This agrees with the shapes of rock fragments shown in Figure 3c. The PPSS fragments under wet testing show a significant reduction of sphericity values. They become flatten with increasing number of test cycles. Their shape is also shown by the images in Figure 3b, where their larger dimensions are parallel to the bedding planes.

Sizes of all fragments remaining in the drum are measured for every 20 cycle interval. They are averaged from three mutually perpendicular axes of the fragment, i.e. longest, intermediate, and shortest. Figure 5 gives normalized fragment size for the three sandstones as a function of test cycle. The fragment size reduction tends to be linear for all test conditions. PPCS and PWSS specimens are highly durable under both wet and dry conditions, where less than 20% of their volume has been losed after 80 test cycles. Rate of size reduction for PPSS specimens are highest. Their volumatic losses are over 40% under dry condition and nearly 80% under wet conditions.

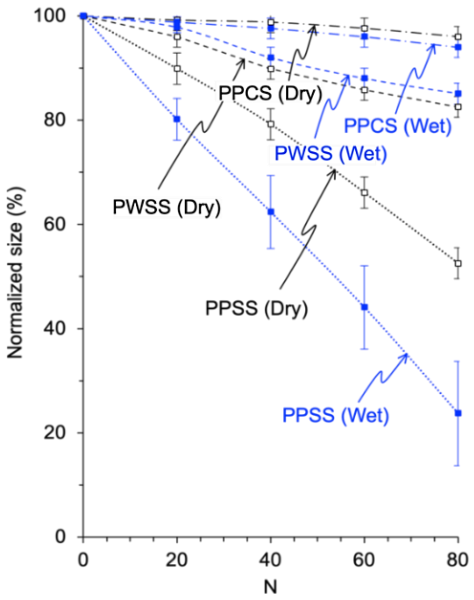

Figure 5 Normalized sizes of fragments remaining in drum as a function of test cycle (N). Open points represent dry testing and solid points represent wet testing

4.2 Passing materials

The passing materials are represented by those smaller than 2 mm (mesh no.10 used for drum openings). To clearly show how the specimens from the three rock types have passed the drum openings, Figure 6 plots accumulated weight percent of passing materials (P_A) from the initial condition through the end of 80 cycles. Exponential equation is proposed to represent the increase of P_A as a function of test cycle (N) for each test condition and rock type:

$$P_A = (\alpha \cdot N) + [1\text{-}exp(-\delta \cdot N)/\beta] \quad (3)$$

where α, β, and δ are empirical constants. Their numerical values are given in Figure 6. Good correlations are obtained (R^2>0.9). The passing weight percents for PWSS specimens under wet and dry conditions tend to be similar. Both PPCS and PPSS specimens show slightly different percentages of passing materials between wet and dry conditions. The passing of PPSS fragments are relatively high within the first 20 cycles (up to 10-20%). They rapidly decrease toward 0.2% near test cycle 80. For PPCS specimens, the dry testing tends to show slightly less passing materials than the wet testing.

Extrapolation of equation (3) to the condition at which all fragments pass through the drum openings (P_A =100%) can predict the number of test cycles needed. The results show that dry and wet testing would require N=219 and 391 for PWSS, 454 and 257 for PPCS, and 135 and 116 for PPSS fragments. These predicted test cycles are later used to calculated the energy required to disintegrate the rocks.

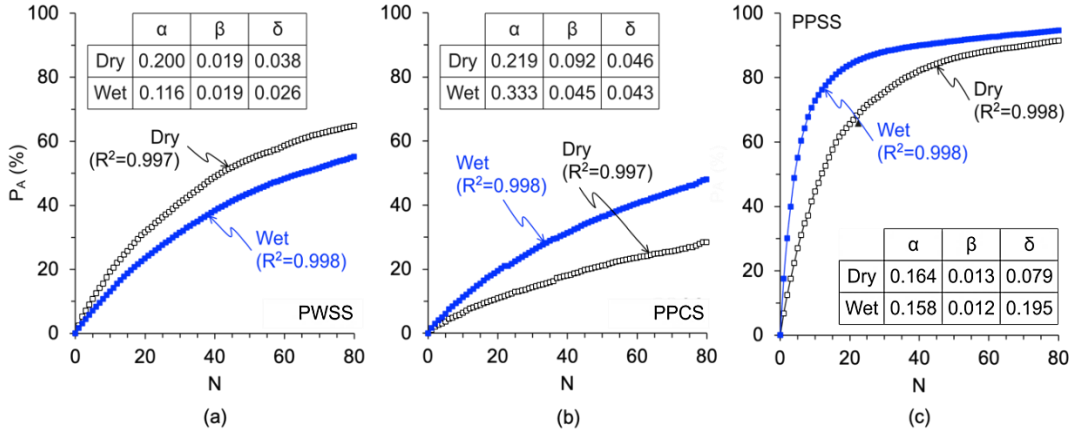

Figure 6 Accumulated weight percent of passing materials (P_A) as a function of test cycle (N). Dry testing (open points) and wet testing (solid points). Lines are fitted by $P_A = (\alpha \cdot N) + [1\text{-}exp(-\delta \cdot N)/\beta]$

4.3 Mineral compositions

X-ray diffraction (XRD) analysis has been performed on rock specimens under initial condition and on those remaining in the drum after 80 cycles. The weight percent of each mineral obtained from the analysis is used to calculate its volumetric percent by following equations:

$$V_i = \{\rho \cdot (W_i/100)/\rho_i\} \cdot 100 \quad (4)$$

where V_i is volumetric percent of each mineral (%),W_i is weight percentage of each mineral obtained from XRD analysis (%), ρ_i is density of each mineral (g/cc), i is number of minerals, and ρ is density of fragments (g/cc). Example of calculation for volumetric percent of quartz content (ρ_i = 2.65 g/cc) in PWSS (ρ = 2.35 g/cc) under initial condition, using Equation (4) and mineral composition obtained from XRD analysis, is shown below:

$$V_i = \{2.35 \cdot (78.58/100) / 2.65\} \cdot 100 = 69.68\ \%. \quad (5)$$

Table 1 shows the results. The mineral compositions for PWSS and PPCS specimens remain effectively unchanged from the initial condition to the end of 80 test cycles. The volumetric reductions of feldspars, mica and clay minerals are observed for the PPSS specimens, particularly under wet testing.

By calculating the mineral compositions in terms of volumetric percent, the porosity (n_c) of fragments can be calculated as follows [33]:

$$n_c = \left\{1 - \left[\sum_{i=1}^{n} \rho \cdot (W_i/100)/\rho_i\right]\right\} \cdot 100 \quad (6)$$

where n_c represents calculated porosity (%) combining connective and non-connective voids. Porosity of PPSS specimens significantly increases after 80 test cycles, where 15% is obtained under dry testing and 16% under wet testing (Table 1). This is supported by the comparable amounts of their mineral compositions and passing materials, as shown in Figure 6(a) and 6(b). This is probably due to the loss of feldspars, mica, and clay minerals, as also reflected by the rapid increase of the passing materials as shown in Figure 6(c). This makes P_A from wet testing higher than that under dry testing. The porosities of PWSS and PPCS specimens remain effectively unchanged for the initial condition and at the end of 80 test cycles under both wet and dry conditions.

Table 1 Mineral compositions in terms of volumetric percent, fragment density (ρ), and calculated porosity (n_c) before testing and after 80 test cycles.

Mineral compositions	PWSS			PPCS			PPSS		
		N=80			*N*=80			*N*=80	
	Initial	Dry	Wet	Initial	Dry	Wet	Initial	Dry	Wet
Quartz	69.68	73.60	74.49	14.24	15.72	11.02	57.86	58.56	56.00
Feldspars	4.53	3.44	3.46	9.86	8.66	9.03	6.40	4.17	2.01
Mica	2.32	1.51	1.31	2.54	2.50	2.90	2.17	1.71	0.98
Clay minerals*	6.25	5.40	4.01	8.28	3.57	6.55	3.15	2.46	1.80
Chlorite	3.74	2.71	3.57	1.98	1.75	1.40	8.59	7.30	11.72
Calcite	0.20	0.17	0.18	58.14	62.79	65.79	11.28	9.59	7.21
Gypsum	0.82	0.23	0.30	2.27	2.37	0.45	2.77	0.00	1.76
Ferrous oxide	0.10	0.05	0.09	1.17	0.41	0.22	1.41	1.54	2.46
ρ (g/cc)	2.35	2.31	2.32	2.67	2.63	2.62	2.53	2.30	2.27
n_c	12.35	12.91	12.57	1.52	2.22	2.63	6.37	14.67	16.05

*Clay minerals are mainly illite, kaolinite and montmorillonite.

5. Energy

An attempt is made here to determine the energy required to reduce the fragment sizes from the initial condition to be less than 2 mm, i.e., all materials passing through the drum openings. The energy defined in this analysis is related to the kinetic energy used by the rocks during drum rotation. This induces rolling of each fragment, leading to the scrubbing and colliding processes between the fragments themselves and between fragments and the inner drum surface.

The kinetic energy consumed by one rock fragment for one revolution can be calculated as [34, 35]:

$$E_i = (1/2)\, I_i \cdot \omega_i^2 \tag{7}$$

where E_i is rotational kinetic energy, I_i is moment of inertia, ω_i is angular velocity, and i is the number of test cycle (varied from 1 to 80). The moment of inertia is obtained by:

$$I_i = (2/5)\, m_i \cdot r_i^2 \tag{8}$$

where m_i is fragment mass during drum rotation and r_i is equivalent radius of fragment under dry testing. The masses of rock fragment for each test cycle are different between dry and wet conditions, where the dry fragment mass can be obtained directly from the measurements at the end of each test cycle. For wet testing, the rock fragment is submerged under water in the trough. Its mass (weight) can be obtained by subtracting the dry mass by the buoyancy force (mass of water with the same volume):

$$m_{i,wet} = m_i - (V_i \cdot \rho_w) \tag{9}$$

where V_i is equivalent volume of fragment at test cycle i and ρ_w is density of water.

The equivalent fragment radius, r_i, can be obtained from the size measurements shown in Figure 5. For example, at initial condition, the equivalent radius is represented by r_0 (i=0) which is equal to 17.37 mm $\{[(28\times28\times28)\cdot(3/4)]^{1/3}\}$. The equivalent volume, V_i, is a representative spherical volume which can be calculated from r_i.

Assuming that there is no sliding between fragment surfaces and inner drum surface, the angular velocity of fragment (ω_i) is equal to that of the drum:

$$\omega_i = v_d / r_d \tag{10}$$

where v_d is linear velocity of drum and r_d is inner drum radius. For one drum revolution, the number of fragment revolutions (R_i) at test cycle i can be calculated by:

$$R_i = r_d / r_i \tag{11}$$

where r_d is inner drum radius which is constant equal to 0.07 m. As a result, the energy used by a fragment for one drum revolution becomes:

$$E_i = [(1/2)\, I_i \cdot \omega_i^2] \cdot R_i \tag{12}$$

And for one test cycle (2,000 drum revolutions):

$$E_i = [(1/2)\, I_i \cdot \omega_i^2] \cdot R_i \cdot 2000 \tag{13}$$

The accumerated energy from test cycles 1 to 80 is

$$E = \sum_{i=0}^{80} E_i \tag{14}$$

The energy results are plotted as a function of test cycle in Figure 7. The diagrams show that rock fragments tested under wet condition consume energy less than those under dry condition. This is primarily because their submerged weight is about 40% less than their dry weight, and results in a reduction of the moment of inertia. The highest energy is used by dry PPCS specimens (Figure 7b) as they have higher density (fragment mass) than the other two sandstones.

Even though the input energy from drum rotation is constant from test cycles 1 to 80, the energy consumed by rock fragments decrease with their sizes, as suggested by non-linear curves of accumulated energy (E) as a function of test cycle (N) in Figure 7. Their relation can be best described by a power equation:

$$E = A \cdot N^B \tag{15}$$

where A and B are empirical constants whose numerical values are given in the figure. Very good correlations are obtained (R^2>0.9). Equation (15) allows predicting the energy that rock fragments consume to become 2 mm or less. By substituting the numbers of test cycles required to obtain 100% passing given in section 4.2, the energy required for each sandstone type and test condition can be calculated. The results are given in Table 2. Disintegration of dry fragments consumes more kinetic energy than that of water submerged fragments. PPCS specimen shows the highest energy consumption than the other two sanstones. Water penetration decreases its kinetic energy used to reduce the fragment size. The discrepansies of the accumulated energy magnitudes between dry and wet testing reflect the role of water penetration. This explains why the PPCS and PPSS specimens show significant differences in energy consumptions between wet and dry, while the water-insensitive PWSS specimens show comparable energy.

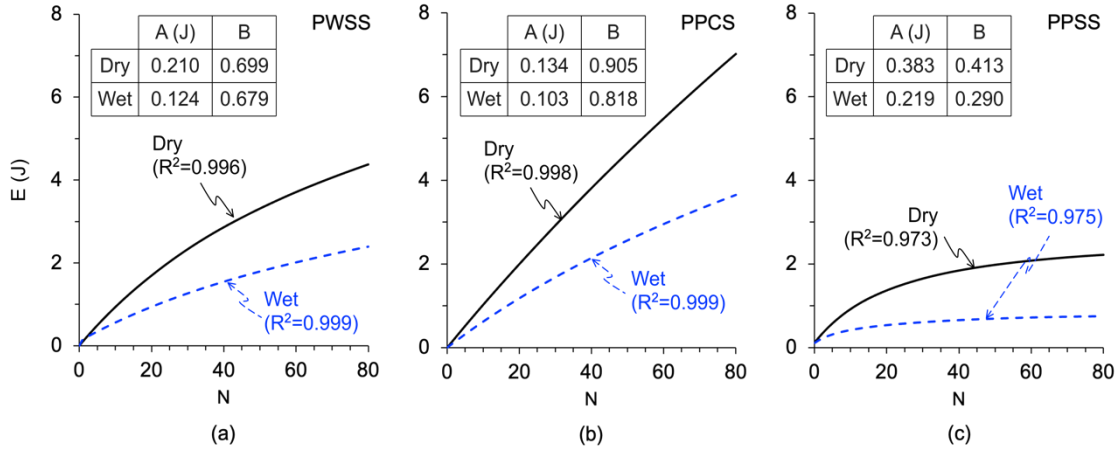

Figure 7 Accumulated energy (E) as a function of test cycle (N). Dry and wet testing shown as solid lines and dash lines. They are fitted by $E=A \cdot N^B$

Table 2 Prediction of accumulated energy (E) and test cycle (N) required to obtain 100% passing materials with 2 mm or less using empirical equation in Figure 7.

Rock types	Conditions	*N*	*E* (J)
Phra Wihan sandstone (PWSS)	Dry	219	9.08
	Wet	391	7.14
Phu Phan conglomeratic sandstone (PPCS)	Dry	454	34.02
	Wet	257	9.64
Phu Phan bedded sandstone (PPSS)	Dry	135	2.90
	Wet	116	0.87

6. Discussions

Modifications of the slake durability index test parameters of ASTM D4644-16 [13] by increasing the drum revolutions from 200 to 2,000 per test cycle and from 2 to 80 cycles provide a clear trend of deterioration for the three sandstones used in this study. The results not only show different deterioration characteristics among different sandstone types, but also allow deriving mathematical representations to predict the number of test cycles required to completely reduce the rock fragment sizes from 28×28×28 mm^3 (gravel [36]) to 2 mm (medium sand) or less. Such extreme modifications have never been attempted elsewhere.

As the test cycles progress, Phu Phan bedded sandstone (PPSS) shows higher roundness values and smaller fragment sizes, as compared to those of PPCS conglomeratic and PWSS sandstones, suggesting that it is more susceptible to erosion than the other two sandstones. All sandstone types and test conditions show the increase of sphericity values, except for the PPSS under wet condition. The reduction of PPSS sphericity is probably due to the separation of bedding planes, which occurs more easily when the fragments are in contact with water. This is supported by the fragment images given in Figure 3(b), where the larger dimensions are parallel to the bedding planes, and by the fragment size reductions shown in Figure 5.

Slaking test induces slightly more deterioration to the PWSS sandstone under dry condition than under wet condition, and results in a higher percentage of passing materials (Figure 6a). This is because scrubbing and colliding effects between fragments are more severe under dry condition. Submersion of the fragments under water in the trough makes them lighter due to their buoyancy forces and reduces fictional resistance between their surfaces. These processes also occur for the PPCS and PPSS sandstones under both test conditions. For these two sandstones, however, water may penetrate into their intergranular boundaries and cementing materials more

easily, and subsequently reduce bonding between the grains. The effect of water penetration for PPCS and PPSS sandstones are predominant over the scrubbing and colliding effects, and hence leading to a higher percentage of passing materials even under wet condition (Figures 6b and 6c). This agrees with the conclusions drawn by Torsangtham et al. [19] who perform a slake durability testing on the same sandstones in Khorat group.

No distinctive change of mineral compositions of the PWSS and PPCS specimens has been observed from their initial condition to the end of 80 test cycles. This is due to the fact that the slaking test performed here is relatively short-term, and hence chemical alterations are unlikely. Small differences of mineral compositions between their initial and test conditions may be due to the intrinsic variability of the rocks. The water-sensitive and soft PPSS sandstone, however, shows notable increases of porosity and reduction of density under both wet and dry conditions (Table 1). This is caused by dislodging of feldspar grains and the initiation of micro-cracks and fissures, particularly along bedding planes during slaking test. The easy separation of bedding planes results in relatively flat fragments with lower sphericity values (Figure 4).

It is recognized that a variety of sandstone types and textures exists in the northeast of Thailand, only three sandstones have been selected for this study. This is limited by research duration and instrumentation. The presented test series require nearly 500 days (3 sandstones × 2 test conditions × 80 test cycles). The test results, nevertheless, provide a clear trend of erosion behavior for each sandstone type and test condition.

It should be noted that the test results obtained here for the Phu Phan and Phra Wihan formations do not represent the erosion behavior of the entire formations. As reported by Murray et al. [29], sandstone formations in Khorat group contain a variety of textures, densities, and compositions, depending upon the depth and location.

The porosity determined here is called “calculated porosity” to avoid confusing with the effective porosity as measured by water saturation method specified by ASTM D7263-21 [30]. The calculated porosity combined connective and non-connective voids in the rock matrix, while the effective porosity represents only connective voids where they can be penetrated and filled by water.

Even though rock fragments are oven-dried at 105°C for 20 hours for each test cycle, the elevated temperature is excluded from the energy calculation. This is based on the experimental results conducted by several researchers who conclude that temperatures of less than 200°C have little effect on rock deterioration and mineral alterations, particularly for sandstones [37-39]. Temperature induces thermal expansion to the minerals composing rocks. Sandstones contain mostly quartz and feldspar whose thermal expansion coefficients are similar [40]. For rocks containing minerals with different thermal properties, such as igneous rocks, the effect of elevated temperature becomes significant.

Under in-situ condition the applied kinetic energy to rock fragments can come under different forms, for examples, falling down from hillside, rolling on stream bed by water flow or on desert floor by wind blow, colliding and scrubbing between fragments, and blasting by water or wind-carried particles. For long-term deterioration (e.g. decades or centuries) chemical energy due to weathering, and mineral alteration and thermal energy by repeating heating and cooling cycles would become more significant. Even though the law of energy conservation is valid, the magnitudes and rates of energy consumption to reduce sandstone fragment sizes under in-situ condition would be difficult to predict. In addition, the site-specific environment where the rock fragments are situated, can change from one period to another. The results obtained here, nevertheless, reveal significant findings that the magnitude and rate of kinetic energy consumption by sandstone fragments depend on fragment size, density, porosity, and rock texture. Large fragments can utilize the applied energy more efficiently than smaller ones, as evidenced by the accumulated passing materials in Figure 6, and by the energy diagrams in Figure 7. Water penetration into fragment matrix helps reducing kinetic energy consumption by weakening the bonding between grains (PPCS specimen) or between bedding planes (PPSS specimen).

7. Conclusions

Conclusions drawn from this experimental and analytical investigation can be summarized as follows.

- Water insensitive Phra Wihan sandstone erodes more quickly under dry condition than under wet condition. Even though it requires longer period to erode under water submersion, due to buoyancy force, it consumes less energy than those under dry condition to reach the same fragment sizes.
- Sandstone with coarser grains and higher density (e.g. Phu Phan conglomeratic sandstone) tends to be more durable than that with finer grains and lower density (e.g. Phra Wihan sandstone), providing that water penetration has insignificant effect during erosion process.
- For sandstones with comparable mineral compositions as tested here, their erosion characteristics are mainly governed by textures, grain sizes, densities, and structures (bedding planes).
- Sandstone fragment roundness and sphericity increase as fragment size decreases. The decrease of fragment sphericity can occur during erosion if bonding along bedding planes is weaker than across the beds, particularly when water penetration occurs.
- Larger sandstone fragments use energy more efficiently to reduce their size than the smaller ones.
- The main mechanisms of sandstone erosion under kinetic energy are scrubbing and colliding processes. These physical processes can, however, be predominated by water penetration, depending upon the rock porosity, density, and bonding between grains.
- The correlation between erosion rate of sandstones and their energy consumption has been proposed. This has never been attempted by other researchers conducted elsewhere. Even though the results are limited to relatively fine grained sandstones, the findings clearly show that the erosion rate of the rocks involves not only their petrographical and mineralogical properties, but also their mechanical and physical bondings, and water penetration.

8. Acknowledgments

This work was supported by Suranaree University of Technology (SUT) and Thailand Science Research and Innovation (TSRI). Permission to publish this paper is gratefully acknowledged.

9. References

[1] Sibille L, Lominé F, Poullain P, Sail Y, Marot D. Internal erosion in granular media: direct numerical simulations and energy interpretation. Hydrol Process. 2015;29(9):2149-63.
[2] Flores AN, Bledsoe BP, Cuhaciyan CO, Wohl EE. Channel-reach morphology dependence on energy, scale, and hydroclimatic processes with implications for prediction using geospatial data. Water Resour Res. 2006;42(6):W06412.
[3] Moses C, Robinson D, Barlow J. Methods for measuring rock surface weathering and erosion: a critical review. Earth-Sci Rev. 2014;135:141-61.
[4] Gupta AS, Seshagiri Rao K. Weathering effects on the strength and deformational behaviour of crystalline rocks under uniaxial compression state. Eng Geol. 2000;56(3-4):257-74.
[5] Erguler ZA, Shakoor A. Relative contribution of various climatic processes in disintegration of clay-bearing rocks. Eng Geol. 2009;108(1-2):36-42.
[6] Torabi-Kaveh M, Mehrnahad H, Morshedi S, Jamshidi A. Investigating the durability of weak rocks to forecast their long-term behaviors. Bull Eng Geol Environ. 2021;81(1):1-22.
[7] Jamshidi A. Slake durability evaluation of granitic rocks under dry conditions and slaking solution and its prediction using petrographic and strength characteristics. Bull Eng Geol Environ. 2023;82(4):1-22.
[8] McCarroll D, Nesje A. Rock surface roughness as an indicator of degree of rock surface weathering. Earth Surf Process Landf. 1996;21:963-77.
[9] Krautblatter M, Moore JR. Rock slope instability and erosion: toward improved process understanding. Earth Surf Process Landf. 2014;39(9):1273-8.
[10] Paripuri PS, Parian M, Rosenkranz J. Breakage process of mineral processing comminution machine-an approach of liberation. Adv Powder Technol. 2020;31(9):3669-85.
[11] Foye WG. Denudation, erosion, corrosion and corrasion. Science. 1921;54:130-1.
[12] Nichols G. Sedimentology and stratigraphy. United Kingdom: Willey-Blackwell; 2009.
[13] ASTM. ASTM D4644-16: Standard test method for slake durability of shale and other similar weak rocks. West Conshohocken: ASTM International; 2016.
[14] Franklin JA, Chandra R. The slake-durability test. Int J Rock Mech Min Sci. 1972;9(3):325-8.
[15] Moradian ZA, Ghazvinian AH, Ahmadi M, Behnia M. Predicting slake durability index of soft sandstone using indirect tests. Int J Rock Mech Min Sci. 2010;47(4): 666-71.
[16] Zhu JJ, Deng H. Durability classification of red beds rocks in central Yunnan based on particle size distribution and slaking procedure. J Mt Sci. 2019;16(3):714-24.
[17] Keaton JR. Estimating erodible rock durability and geotechnical parameters for SCOUR analysis. Environ Eng Geosci. 2013;19(4):319-43.
[18] Shahid MR. Evaluation of multivariable regression in predicting rock slake durability index. SRPH J Fundam Sci Technol. 2022;4(1):1-20.
[19] Torsangtham P, Khamrat S, Thongprapha T, Fuenkajorn K. Laboratory assessment of long-term durability of some decorating and construction rocks. Eng J Res Dev. 2019;30(3):135-43.
[20] Fereidooni D, Khajevand R. Correlations between slake-durability index and engineering properties of some travertine samples under wetting-drying cycles. Geotech Geol Eng. 2018;36:1071-89.
[21] Walsri C, Sriapai T, Phueakphum D, Fuenkajorn K. Simulation of sandstone degradation using large-scale slake durability index testing device. Songklanalarin J Sci Technol. 2012;34(5):587-96.
[22] Azhar MU, Zhou H, Yang F, Younis A, Lu X, Houguo F, et al. Water-induced softening behavior of clay-rich sandstone in Lanzhou Water Supply Project, China. J Rock Mech Geotech Eng. 2020;12(3):557-70.
[23] Erguler ZA, Ulusay R. Assessment of physical disintegration characteristics of clay-bearing rocks: disintegration index test and a new durability classifi-cation chart. Eng Geol. 2009;105(1-2):11-9.
[24] Yan L, Liu P, Hua P, Kasanin-Grubin M, Lin K. Laboratory study of the effect of temperature difference on the disintegration of redbed softrock. Phys Geogr. 2019;40(2):149-63.
[25] Sousa LMO, Surarez del Rio LM, Calleja L, Ruiz de Argandoña VG, Rey AR. Influence of microfractures and porosity on the physico-mechanical properties and weathering of ornamental granites. Eng Geol. 2005;77(1-2):153-68.
[26] Corominas J, Martinez-Bofill J, Soler A. A textural classification of argillaceous rocks and their durability. Landslides. 2015; 12(4):669-87.
[27] Heidari M, Momeni AA, Rafiei B, Khoodabakhsn S, Toorabi-Kaveh M. Relationship between petrographic characteristic and the engineering properties of Jurassic sandstones, Hamedan, Iran. Rock Mech Rock Eng. 2013;46:1091-101.
[28] Hawkins AB, McConnell BJ. Sensitivity of sandstone strength and deformability to changes in moisture content. Q J Eng Geol Hydrogeol. 1992;25(2):115-30.
[29] Murray C, Heggemann H, Gouadain J, Krisadasima S. Geological history of the siliciclastic Mesozoic strata of the Khorat Group in the Phu Phan range area, northeastern Thailand. International Symposium on Biostratigraphy of Mainland Southeast Asia: Facies and Paleontology; 1993 Feb; Chiang Mai, Thailand. p. 23-49.
[30] ASTM. ASTM D7263-21: Standard test methods for laboratory determination of density and unit weight of soil specimens. West Conshohocken: ASTM International; 2021.
[31] ASTM. ASTM E3294-22: Standard guide for forensic analysis of geological materials by powder X-Ray diffraction. West Conshohocken: ASTM International; 2022.
[32] Hryciw RD, Zheng J, Shetler K. Particle roundness and sphericity from images of assemblies by chart estimates and computer methods. J Geotech Geoenviron Eng. 2016;142(9):0001485.
[33] Chamwon S, Thongprapha T, Fuenkajorn K. Correlation between ultrasonic pulse velocities and physical and chemical properties of rocks. Proceedings of Academicsera International Conference; 2020 Dec 6-7; Pattaya, Thailand.
[34] Meriam JL, Kraige LG. Engineering mechanics volume 1: statics. Fluid statics. New York: John Wiley & Sons; 1980.
[35] Meriam JL, Kraige LG. Engineering mechanics volume 2: dynamics. Kinetics of particles. New York: John Wiley & Sons; 1980.
[36] ASTM. ASTM D2487-17: Standard practice for classification of soils for engineering purposes (Unified Soil Classification System). West Conshohocken: ASTM International; 2017.

[37] Brotons V, Tomas R, Ivorra S, Alarcon JC. Temperature influence on the physical and mechanical properties of a porous rock: San Julian's calc-arenite. Eng Geol. 2013;167:117-27.
[38] Li M, Liu X. Effect of thermal treatment on the physical and mechanical properties of sandstone: insights from experiments and simulations. Rock Mech Rock Eng. 2022;55(6):3171-94.
[39] Sirdesai NN, Mahanta B, Ranjith PG, Singh TN. Effects of thermal treatment on physico-morphological properties of Indian fine-grained sandstone. Bull Eng Geol Environ. 2019;78(2):883-97.
[40] Somerton WH. Thermal properties and temperature-related behavior of rock/fluid systems. Amsterdam: Elsevier; 1992.